academicJournals

Vol. 6(3), pp. 15-33, August 2015
DOI 10.5897/JCEMS2015.0212
Articles Number: 8F82FDC54973
ISSN 2141-6605

http://www.academicjournals.org/JCEMS

Journal of Chemical Engineering and Materials Science

Full Length Research Paper

Comparison between mixing and shaking techniques during the destabilization-hydrolysis of the acid mine drainage (AMD) using $Ca(OH)_2$ and $Mg(OH)_2$

Ntwampe, I. O.*, Waanders, F. B. and Bunt T. S. S. R.

School of Chemical and Minerals Engineering, North-West University, Potchefstroom Campus, Private Bag X6001, Potchefstroom 2520, South Africa.

Received 3 March, 2015; Accepted 22 July, 2015

Acid mine drainage (AMD) is detrimental to both humans and the ecosystem, and contains sulphuric acid and heavy metals, which have to be removed by dosing the coagulants. A 200 mL sample of AMD, emanating from a mining area in South Africa was poured into 500 mL glass beakers or Erlenmeyer flasks and were dosed with 0.043 M $Ca(OH)_2$, 0.043 M $Mg(OH)_2$ and synthetic 0.043 M $CaMg.2(OH)_2$ and treated in a jar test or shaking apparatus employing rapid agitation at 250 rpm for 2 min. Each batch of samples was allowed to settle for an hour after which the pH, conductivity and turbidity were measured. The results showed that the turbidity removal efficiency exhibited by $Ca(OH)_2$ or $Mg(OH)_2$, and synthetic $CaMg.2(OH)_2$ dosage of a range 30 to 60 mL was identical all above 90%. Effective wastewater treatment is not necessarily dependent upon the pH but the ability of the coagulant to destabilize the double layer (high electronegativity) of the aqua-colloids coupled with optimal hydrolysis, precursor to adsorption. The Ca^{2+} and Mg^{2+} ions added to AMD sample do not only neutralize the solution, but also cause destabilization; whereas the anionic species (OH^-) increases the pH of the system. The Ca^{2+} and Mg^{2+} ions in $Ca(OH)_2$ and $Mg(OH)_2$ added to AMD sample respectively did not only neutralize the solution, but also cause destabilization, whereas the unreacted OH^- ions increase the pH of the system. The identical turbidity removal yielded by all reagents confirms that the $CaMg2(OH)_2$ can be used as a replacement of $CaMg(CO_3)_2$. Turbidity removal in AMD sample with $Ca(OH)_2$, $Mg(OH)_2$ or $CaMg.2(OH)_2$ dosages is of a physical nature as can be observed from the SEM images, showing sponge cake-like structure with dense flocs linked together.

Key words: Coagulants, shaking, agitation, settle, pH, turbidity.

INTRODUCTION

Wastewater in the form of uncontrolled drainage, poses a serious environmental catastrophe world-wide. Acid mine drainage (AMD) forms part of this uncontrolled wastewater because it can either be formed during or after mining, where it flows into any water-course. The AMD is detrimental to the environment because of high sulphur content which is converted to sulphuric acid after the oxidation of its main constituent, ferrous or ferric sulphites (FeS_x).

These are naturally occurring compounds underground,

*Corresponding author. E-mail: ontwampe@gmail.com.

and pyrite (FeS_2) is a common species and a main attribute to AMD after oxidized in an aqueous medium (Equation 1).

$$2\ FeS_2 + 7\ O_2 + 2\ H_2O \rightarrow 2\ Fe^{2+} + 4\ SO_4^{2-} + 4\ H^+ \quad (1)$$

The Fe^{2+} ions may further be oxidized to form Fe^{3+}, which act as a reducing agent to oxidize the residual Fe^{2+} (Equation 2), thus increasing the SO_4^{2+} content in the solution (AMD) (Equation 1)

$$FeS_2 + 14\ Fe^{3+} + 8\ H_2O \rightarrow 15\ Fe^{2+} + 2\ SO_4^{2-} + 16\ H^+ \quad (2)$$

The AMD is formed when the pyrite is oxidized in the presence of water and oxygen to form acidic, sulphate-rich drainage. Metal contamination associated with AMD depends upon the type and amount of sulphide mineral oxidized, as well as the type of gangue minerals present in the rock (Diz, 1997). There are other sulphide containing minerals such as pyrrhotite (FeS), chalcocite (CuS) and galena (PbS) (Kalin et al., 2006). Biological formation of AMD includes the oxidation of pyrite by bacteria, namely *Acidithiobacillus ferrooxidants* to form sulphuric acid as shown by Equation 9. The dumping sites also play as the source of AMD which occurs when the dumps with high permeability are associated with high oxygen ingress, which then contributes to higher chemical reaction rates. Higher temperatures cause increased oxygen ingress through convection. These bacteria may also accelerate oxidation of sulphides of antimony, gallium, molybdenum, arsenic, copper, cadmium, cobalt, nickel, lead and zinc. The *A. ferrooxidants* bacteria are most active in water with a pH of less than 3.2. If conditions are not favourable, the bacterial influence on acid generation will be minimal (Diz, 1997). Abandoned mines also contribute towards AMD when they are flooded with groundwater which can re-enter the catchment areas by means of the adits. These waters are rich in sulphates and dissolved metals and have an acidic pH due to the oxidation of the sulphide containing minerals. When the Fe^{2+} ions (Equation 2) have been oxidized to form Fe^{3+} ions and saturation point has been reached, the latter undergo hydrolysis reaction and precipitates (flocs) are formed as shown by Equation 3.

$$Fe^{3+}_{(aq)} + 3\ H_2O_{(aq)} \rightarrow Fe(OH)_{3(s)} + 3\ H_{(aq)}^{+} \quad (3)$$

Other sources of AMD from the gold mining industry are derived from the sand and slime dams resulting from tailings. The residual sulphides found in these dumps are oxidized when reacting with O_2 and rainwater. The oxidation acidifies the percolating water, which is also believed to enter streams (Kalin et al., 2006; Naicker et al., 2003). Researchers such as Semerjian and Ayoub (2003), Watten et al. (2005), Akcil et al. (2006), Kurniawan et al. (2006), Herrera et al. (2007) and Sibrell et al. (2009) conducted studies on AMD employing lime neutralization for the removal of sulphates. New techniques have been explored, but most of them are either costly or selective in wastewater of certain qualities. Several new processes have been developed, based on the use of precipitated calcium carbonate or lime pre-treatment for neutralization of AMD and partial desalination (Scherrenberg et al., 2008; Maree et al., 2004b; Chang and Yu, 2004; Carballa et al., 2005; Hankins, 2006; Pratt et al., 2007; Edwards and Withers, 2007; Kempkes et al., 2007; Suarez et al., 2009; van der Graaf et al., 2010; Jiang et al., 2012).

According to various technologies exploited in AMD treatment, most of the approaches conducted by Goldberg (2002), Metcalf et al. (2003), Sincero and Sincero (2003), McCurdy et al. (2004), Swartz et al. (2004), Amuda et al. (2006), Ghaly et al. (2006) and Aubé (2004) focus more on the physico-chemical properties of the colloidal suspension, whereas the effectiveness of the treatment mainly relies on the reaction dynamics between the colloidal suspension and coagulants. Effective performance of destabilization depends primarily upon the type of colloids, hydrophilic (water-loving) or hydrophobic (water-hating), the physico-chemical properties of the coagulant(s) and the intensity of the mechanical agitation for the dispersion of the coagulant(s) throughout the colloidal suspension (Li and Hoggins, 2010). Other solute properties include solute partition coefficient, polarizability and molecular structure influence pollutants adsorption (Bolto, 2007; Adams et al., 2002; de Ridder et al., 2010). Those which are associated with the coagulants include electronegativity, charge per surface area, valence electron, particle size, porosity, density (Wulfsberg, 1987). It is also essential that the concentration of the coagulants must be sufficient to rapidly precipitate the metals in the colloidal suspension to form metal hydroxide species (precipitates) with high settling velocity for settling and enmeshment of the colloidal particles in these precipitates. The effectiveness of coagulation depends upon the change in ionic concentration, and it increases exponentially as the charge of the ions increases (Jiang et al., 2012; Dey et al., 2004).

Mechanical agitation (mixing or shaking) plays a pivotal role during destabilization-hydrolysis of wastewater by inducing a velocity gradient (du/dy), that is, a change of velocity per change of distance and disperses the reagents collision throughout the solution. The type of coagulant (physico-chemical properties) which is dosed and the time taken during mixing, determine the optimum velocity gradient (Metcalf et al., 2003; Sincero and Sincero, 2003; McCurdy et al., 2004; Swartz et al., 2004; Amuda et al., 2006; Ghaly et al., 2006). As mixing progresses, destabilization-hydrolysis-aggregation occurs due to the physico-chemical reactions which take place in the system. All these reactions occur during coagulation

and flocculation stages. The former occurs within a very short space of time during rapid mixing whereas the latter during slow mixing. Primary flocs are formed during coagulation and enlarge into secondary larger flocs during flocculation process due to (Swartz et al., 2004).

A treatment system with effective correlation of coagulant/flocculent-colloidal particle dispersion yields the best destabilization-hydrolysis results, which also enhance subsequent reactions. Destabilization occurs after the addition of the reagents when the equilibrium state of the colloidal suspension is disturbed (Aboulhassan et al., 2006; Aguilar et al., 2002; Aguilar et al., 2005). The rate of destabilization determines the rate of flocs formation during coagulation and flocculation. The effectiveness of the process depends upon the ionic strength of the coagulants added to the solution to disturb equilibrium between van der Waals forces of attraction, electrostatic forces of repulsion and hydrodynamic forces (Binnie et al., 2003). Collision rate plays a pivotal role in the formation of the larger flocs because excessive shear force can result in rupturing of the flocs to restabilize (Tchobanoglous et al., 2003; Swartz et al., 2004), which is also caused by overdosing (van Nieuwenhuijzen, 2002). Atkins and de Paula (2006) stated that the collision efficiencies of hydrodynamic forces for various size ratios of particles involved in the collision and the predicted results show the comparison on curvilinear and rectilinear models as follows:

i. Collision frequencies are less than 0.5 s^{-1} in perikinetic flocculation.
ii. Collision frequencies are less than 5 s^{-1} in orthokinetic flocculation.
iii. Collision frequencies are in a range of 2 - 3 s^{-1} or less for differential sedimentation.

On the other hand, the observations on the flocculation and sedimentation are also as below:

i. Perikinetic flocculation dominated when the secondary particle was less than 1 mm,
ii. Differential sedimentation dominated when the secondary particle is greater than 10 mm,
iii. For both orthokinetic flocculation and differential sedimentation, the collision frequency was a strong function of particle size, dominated by the diameter of the larger particles.

Since the rate of the collision frequencies is influenced by the intensity of mixing, the source has not been subjected to high shear forces (Binnie et al., 2003). It is very essential to optimize the velocity gradient of the system to avoid restabilization due to flocs rupture, a parameter which is common to both mixing and shaking mechanisms. When mechanical agitation is optimal, the particles maintain their original sizes and collide effectively to form larger flocs during perikinetic or orthokinetic floc formation (Water Specialist Technology, 2003). During perikinetic floc formation, the particles collide as a result of Brownian motion whereas orthokinetic floc formation occurs when particles collide due to dissipation of mixing energy. The decrease in the number of spherical particles to form larger flocs during collision, as a function of time is expressed as:

$$-\frac{dn}{dt} = \alpha \frac{4KT}{3\mu} n^2 \quad (4)$$

where n = total number of particles per unit water volume, α = collision efficiency, K = Boltzman constant, T = absolute temperature and μ = dynamic water viscosity.

During mixing, the collision of the frequency of the particles is artificially increased, and the decrease in the number of particles as a function of time is expressed by Equation 5.

$$-\frac{dn}{dt} = \frac{4}{3} \alpha . n_1 . n_2 . R^3 . G_v \quad (5)$$

where n_1 = number of particles with diameter d_1, n_2 = number of particles with diameter d_2, R_v = collision radius $(0.5.d_1+d_2)$ and G_v = velocity gradient for floc formation.

The velocity gradient (floc formation), as indicated that it plays a pivotal role in maintaining the particles' diameter unchanged during stirring (Sincero and Sincero, 2003), is expressed by Equation 6.

$$G_v = \sqrt{\frac{\rho g \Delta H}{\mu . \tau c}} \quad (6)$$

where τ_c = residence time in the mixing zone, ΔH = head loss of mixing tank, ρ = density of water, g = gravity.

The parameters which have been applied in Equations 1 to 3 are influenced by the type of the mechanical method employed, either mixing or shaking, hence it is essential to disperse the coagulants/flocculent with minimum shear forces during destabilization-hydrolysis to eliminate flocs rupture.

Table 1 shows some of the physico-chemical properties of the coagulants which play a pivotal role in the destabilization-hydrolysis during wastewater treatment. When the choice of an ideal coagulant/flocculent and an appropriate solution dispersing method has been selected, the treatment is prone to yield effective destabilization-hydrolysis reaction. The former includes the disturbance of the equilibrium between the van der Waals forces of attraction and electrostatic repulsive forces in the colloidal suspension, whereas hydrolysis is the formation of the metal hydroxide species (Sincero and Sincero, 2003), as shown by Equation 7.

$$M^{n+} + n\ H_2O \rightleftharpoons M(OH)_{n(s)} + n\ H^+ \quad (n= \text{valence and } M = \text{metal}) \quad (7)$$

Table 1. Physico-chemical properties of Ca and Mg atoms.

Metal	Radius (pm)	χ_p	Z^2/r (pm^{-1})	Max oxid No.	pk_b
Ca	197	1.0	0.020	2	1 - 6
Mg	160	1.31	0.025	2	1 - 6

During hydrolysis, there is a change in the concentrations of the metal ions of a salt or hydroxide to form various species at specific pH values which can be represented mathematically as:

$$\frac{\partial C}{\partial t} = k[\frac{\partial 2C}{\partial x 2} + \frac{\partial 2C}{\partial y 2} + \frac{\partial 2C}{\partial z 2}] \quad (8)$$

Destabilization can be classified into four categories such as double layer compression, neutralization, particle bridging and entrapment in a precipitate (Sincero and Sincero, 2003). These types of destabilization depend upon the type of the coagulant(s). AMD is the type of wastewater which is investigated in this study using $Ca(OH)_2$, $Mg(OH)_2$ and synthetic $CaMg.2(OH)_2$ as coagulants. The latter was synthesized using 50% molar concentration of Ca^{2+} and Mg^{2+} each compared to 100% molar concentration of Ca^{2+} or Mg^{2+} ions in their metal hydroxides. The objective to conduct this set of experiment was to compare the destabilization-hydrolysis potential of the hydroxides of Ca and Mg dosed in the AMD sample respectively, and as combined $CaMg.2(OH)_2$ using mixing or shaking techniques. The rationale is to determine the viability of replacing mixing with shaking to avoid rupturing of the flocs due to shear stress inevitable in rapid mixing as stated by Freeze et al. (2001), Aysegul and Enis (2002), Sincero and Sincero (2003), McCurdy et al. (2004), Swartz et al. (2004) and Ghaly et al. (2006). A synthetic metal hydroxide of a combination of Ca and Mg has never been used in AMD treatment, and is intended to replace dolomite which has exhibited that a certain dosage of less than 150 mL of its particle size takes more than 6 h to decrease the concentration of ferric ions to near completion, and also its relatively insolubility at pH values greater than 7 (Maree et al., 2004a). The replacement of $Ca(OH)_2$ with $Mg(OH)_2$ is to avoid the reaction of Ca^{2+} and SO_4^{2+} to form gypsum ($CaSO_4.2H_2O$). The $Mg(OH)_2$ behaves as a softener, OH^- donor to the colloidal suspension for metal hydroxides formation and adsorption of the metals onto the surface of $Mg(OH)_2$ particles. It produces a faster settling rate for metal hydroxide flocs as well as a denser sludge (Fu and Wang, 2010), compared to $Ca(OH)_2$. This occurs because of the lower solubility of $Mg(OH)_2$ (k_s of 1.5×10^{-11}), resulting in a slower release of the OH^- ion into the solution, with a higher rate of precipitation (Wang et al., 2004).

According to the hydrolysis of the $FeCl_3$ (Equation 3), the protons which are released react with the metal hydroxide ($CaMg.2(OH)_2$) to form Mg^{2+} (Equation 9), which will further exchange the OH^- with $Ca(OH)_2$ to form insoluble $Mg(OH)_2$ (Equation 11).

$$6\ H^+ + 3\ Mg(OH)_2 \rightarrow 3\ Mg^{2+} + 6\ H_2O \quad (9)$$

$$2\ Fe^{2+} + ½\ O_2 + 2\ H^+ + 3\ Mg(OH)_{2(s)} \rightarrow 2\ Fe(OH)_{3(s)} + 3\ Mg^{2+} + H_2O \quad (10)$$

$$Mg^{2+} + Ca(OH)_2 \rightarrow Mg(OH)_{2(s)} + Ca^{2+} \quad (11)$$

$$SO_4^{2-} + Ca^{2+} + 2\ H_2O \rightarrow CaSO_4.2H_2O \quad (12)$$

On the other hand, the Fe^{2+} is oxidized by O_2 in aqueous environment to form Fe^{3+} (in Equation 10), which is hydrolysed to form $Fe(OH)_3$ precipitate. The $Mg(OH)_2$ added to AMD then neutralizes the acid (H^+) to form soluble Mg^{2+} and H_2O (Equation 9). The $Ca(OH)_2$ reacts with Mg^{2+} to form Ca^{2+} ions and $Mg(OH)_2$ precipitates (Equation 11), and the Ca^{2+} reacts with the sulphides to form $CaSO_4.2H_2O$ precipitates (gypsum) (Equation 12). The rate of sulphate removal by gypsum crystallization may be predicted from Equation 12 (Maree et al., 2004).

$$d[CaSO_4.2H_2O]/dt = k[CaSO_4.2H_2O](S)[C-C_0]^2 \quad (13)$$

where $d[CaSO_4.2H_2O]/dt$ = rate of crystallisation, k = reaction rate constant, $[CaSO_4.2H_2O](S)$ = surface area of the seed crystals, C = initial concentration of calcium sulphate in solution, and C_0 = saturated concentration of calcium sulphate in solution.

The concentration of Ca^{2+} (Equation 9) in the AMD can be used to determine the removal of the sulphites which were converted to sulphates (Equation 9). In this study, the destabilizing-hydrolysis potential of 0.043 M of the metal ions of $Ca(OH)_2$, $Mg(OH)_2$ and $CaMg.2(OH)_2$, in a highly acidic AMD sample using a jar test and a shaker at 250 rpm is investigated. The turbidity removal efficiency is a determinant on the degree of destabilization of the double layer (Figure 1) is affected by the afore-mentioned coagulants. The study also aims to determine the effect of both cationic and anionic components of the metal hydroxide in destabilization-hydrolysis.

MATERIALS AND METHODS

In this study, coagulation-flocculation treatment has been applied to AMD solution using 0.043 M Ca^{2+} in $Ca(OH)_2$, 0.043 M Mg^{2+} in $Mg(OH)_2$, or a combination of 0.021 M Ca^{2+} and 0.021 Mg^{2+} in $Ca(OH)_2$ and $Mg(OH)_2$ respectively to form 0.043 M $CaMg.2(OH)_2$

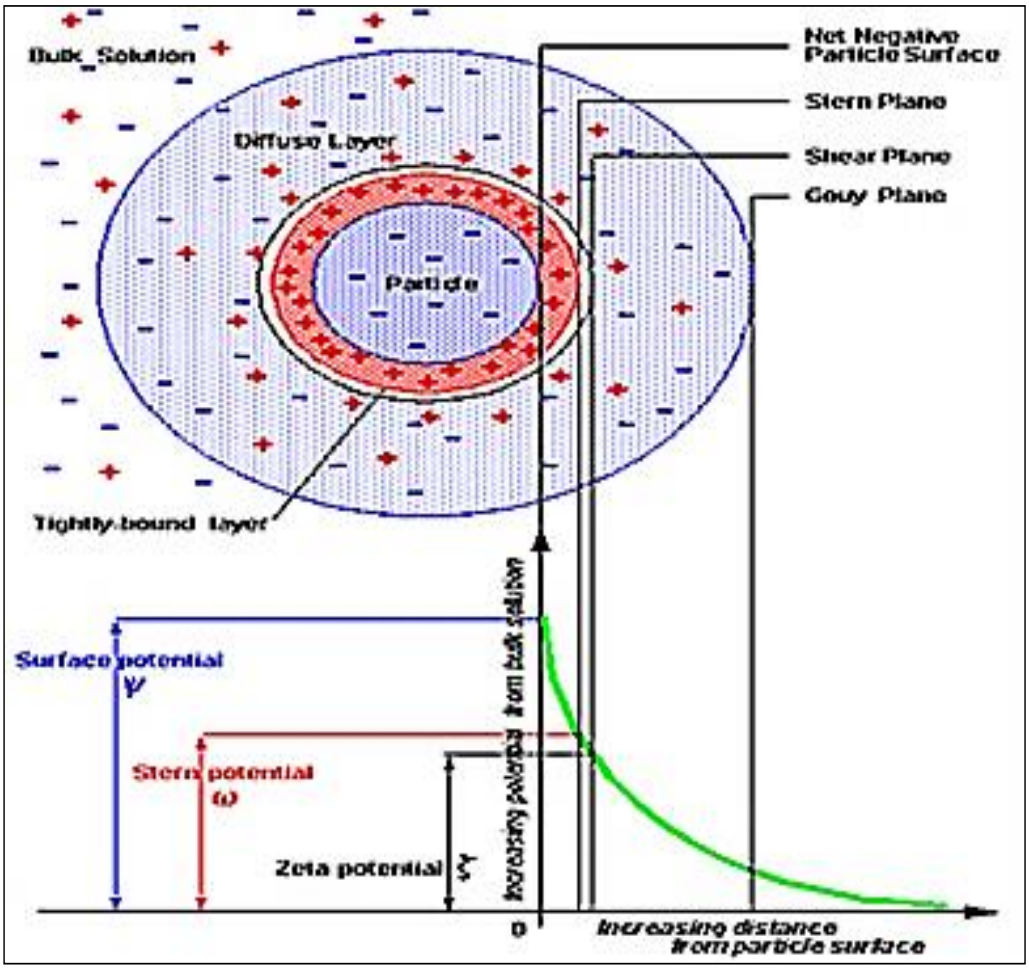

Figure 1. A hydrated colloid showing double layer.

using a jar test or a shaker. The pH, conductivity and turbidity of the samples were measured before the jar test. The samples were placed in a flocculator with rapid mixing at 250 rpm for 2 min. The samples were allowed to settle for 1 h and thereafter the pH, conductivity and turbidity were measured. A second similar experiment was conducted in a shaker at 250 rpm for 2 min. The samples were allowed to settle for 1 h and thereafter the pH, conductivity and turbidity were measured.

The novelty in this study is to determine the turbidity removal potential of the $Mg(OH)_2$ or a synthetic $CaMg.2(OH)_2$ polymer as a possible replacement of an environmentally hazardous $Ca(OH)_2$ or $CaMg(CO_3)_2$. The second novelty includes the comparison of the efficiency in the turbidity removal when the AMD sample is treated with mixing and shaking.

Acid mine water sample

The samples were collected from the Western Decant near Krugerdorp in twenty-five litres plastic drum. The samples were "air-tied" and stored at room temperature. The pH, conductivity and turbidity of the AMD solution were 2.56, 4.43 mS/cm and 100 NTU, respectively. The solid content of the sample was 6.8 g in a 200 mL AMD sample. The sample contained the following major elements: Cu, Zn, Co, Ni, Mn, Ti, Pb, Al, Fe, Li, Sb, Se, Na, Mg, Ca and K, and the concentrations are shown in Table 2.

Coagulants

The concentration of the metal hydroxide of 0.043 M of Ca^{2+} in $Ca(OH)_2$, 0.043 M Mg^{2+} in $Mg(OH)_2$, or a combined 0.043 M Ca^{2+}/Mg^{2+} in $CaMg.2(OH)_2$ as used in this study was chosen as per a study which was conducted by Fasemore (2004) on paint wastewater treatment.

The calculation of the mass of metal salt to obtain 0.043 M of M^{3+} (M^{2+} = Ca or Mg) is as follows:

a. $Ca(OH)_2$ or $Mg(OH)_2$ or $CaMg.2(OH)_2$

0.043 M of M^{3+} × mass of $M^*(OH)_2$ (M^* = Ca or Mg) (14)

b. $CaMg.2(OH)_2$

0.021 M of M_1^{2+} + 0.021 M of M_2^{2+} x $M_1M_2(OH)_2$

(M_1 = Ca and M_2 = Mg) (15)

Table 2. Printout of mineral content in untreated AMD sample of IC analyses.

Solution label	Element	Conc	Units
Sample 1	Al 396.152	1.17129	ppm
Sample 1	Ca 422.673	182.128	ppm
Sample 1	Co 230.786	0.133436	ppm
Sample 1	Cu 327.395	0.142323	ppm
Sample 1	Fe 259.940	28.3576	ppm
Sample 1	K 766.491	4.59173	ppm
Sample 1	Mg 280.270	67.3925	ppm
Sample 1	Mn 257.610	35.3678	ppm
Sample 1	Na 588.995	44.572	ppm
Sample 1	Ni 231.604	0.443153	ppm
Sample 1	Pb 220.353	0.605979	ppm
Sample 1	Sb 206.834 uv	0.270407	ppm
Sample 1	Se 196.026 uv	0.711199	ppm
Sample 1	Zn 213.857	0.348886	ppm

Printout of mineral content in untreated AMD sample of IC analyses (5 × dilution).

Table 3. Diprotic metal hydroxide dosed into AMD sample.

Salt	Mass of salt (g)	Concn (mol/L)	M^{3+}concn (mol/L)
$Ca(OH)_2$	3.18	0.043	0.043
$Mg(OH)_2$	2.49	0.043	0.043
$CaMg.2(OH)_2$	4.23	0.043	0.043

Table 3 shows monoprotic, diprotic metal salts and metal hydroxide dosed into AMD.

EXPERIMENTS

Jar test procedure

The equipment used for the jar tests was a *BIBBY Stuart Scientific Flocculator (SW1 model)*, which has six adjustable paddles with rotating speeds between 0 to 250 rpm. The AMD solution containing 6.8 g colloid in 200 mL of the solution was poured in each of the five 500 mL glass beakers for the test. Different dosages of 0.043 M Ca^{2+} or 0.043 M Mg^{2+} in $Ca(OH)_2$ and a combination of 0.021 M Ca^{2+} and 0.021 M Mg^{2+} in $Mg(OH)_2$ in $CaMg.2(OH)_2$ or $CaMg(OH)_2$ were added to the AMD samples. The experiments were conducted employing rapid mixing or shaking (250 rpm for 2 min). The rationale was to determine a correlation between the pH changing trend and turbidity removal when the treatment is conducted in acidic wastewater through neutralization.

The experiments were conducted in the following order: In the first set of experiments, the samples used had varying dosages of $Ca(OH)_2$ and treated in two different methods such as mixing in a jar test and shaken. A second similar set of experiments was carried out by replacing the $Ca(OH)_2$ with $Mg(OH)_2$. A third similar set of experiments was carried out by replacing the $Mg(OH)_2$ with $CaMg.2(OH)_2$. An extra similar set of experiments was conducted by replacing $CaMg.2(OH)_2$ with $CaMg(OH)_2$. After rapid mixing or shaking as afore-mentioned, the samples in all the sets of experiments were allowed to settle for 1 h, after which the pH, conductivity and turbidity were measured.

Performance evaluation

The pH was used as a determinant to assess the rate of hydrolysis and hydrolytic potential of the coagulants at different mixing duration, whereas turbidity was measured to determine the removal of colloidal particles from the samples.

pH measurement

A Metter Toledo Seven Multimeter (made in Germany) pH meter with an electrode filled with silver chloride solution and the outer glass casing with a small membrane covering at the tip was used. The equipment was calibrated with standard solutions with the pH of 4.0 and 7.0 before use.

Turbidity measurement

A Merck Turbiquant 3000T Turbidimeter (made in Japan) was used to determine turbidity or the suspended particles in the supernatant using NTU as a unit of measurement. It was calibrated with 0.10, 10, 100, 1000 and 10000 NTU standard solutions.

Inductively coupled plasma (ICP)

A Perkin Elmer Optima DV 7000 ICP-OES Optical Emission Spectroscopy (made in USA) was used to determine the metals in the supernatant using ppm as a unit of measurement. It was calibrated with the standard solution between 2 to 50 ppm of the salts mentioned in this study.

Table 4. Ionic strength of Ca and Mg atoms.

Species	Ionic strength
Ca^{2+} in $Ca(OH)_2$	0.194
Mg^{2+} in $Mg(OH)_2$	0.176

Table 5. Printout of mineral content in AMD sample as obtained from IC analyses.

Solution label	Element	Conc	Units
Sample 3	Al 396.152	1.78164	ppm
Sample 3	Ba 455.403	0.018757	ppm
Sample 3	Ca 422.673	160.373	ppm
Sample 3	Co 230.786	0.118617	ppm
Sample 3	Cu 327.395	0.253451	ppm
Sample 3	Fe 259.940	34.8077	ppm
Sample 3	K 766.491	4.66202	ppm
Sample 3	Mg 280.270	85.4535	ppm
Sample 3	Mn 257.610	28.7752	ppm
Sample 3	Na 588.995	41.174	ppm
Sample 3	Ni 231.604	0.396473	ppm
Sample 3	Sb 206.834 uv	0.114622	ppm
Sample 3	Zn 213.857	0.536304	ppm
Solution label	**Element**	**Conc**	**Units**
Sample 5	Al 396.152	1.27288	ppm
Sample 5	Ca 422.673	147.223	ppm
Sample 5	Co 230.786	0.12674	ppm
Sample 5	Cu 327.395	0.202624	ppm
Sample 5	Fe 259.940	32.4392	ppm
Sample 5	K 766.491	4.03479	ppm
Sample 5	Mg 280.270	83.4335	ppm
Sample 5	Mn 257.610	28.726	ppm
Sample 5	Na 588.995	37.571	ppm
Sample 5	Ni 231.604	0.423145	ppm
Sample 5	Sb 206.834 uv	0.111941	ppm
Sample 5	Se 196.026	0.962263	ppm
Sample 5	Zn 213.857	0.538141	ppm

Sample 3 = concentration of AMD samples in experiment (A) and sample 5 = concentration of AMD samples in experiment (B). Printout of mineral content in AMD sample as obtained from IC analyses (5 × dilution).

RESULTS AND DISCUSSION

According to Equation 1, the ratio of Fe^{2+} to H^+ is 1:2, and the concentration of the hydrogen $[H^+]$ in AMD sample (Equation 1) at a pH of 2.56 is 2.75×10^{-3} M. The concentration of Fe^{2+} $[Fe^{2+}]$ is therefore 1.37×10^{-3} M, where of SO_4^{2+} $[SO_4^{2-}]$ is also 2.75×10^{-3} M. The reduced minerals in AMD sample after treatment are shown in Table 5.

Figure 2 shows the pH changing trend in the AMD sample with the added coagulants ($Ca(OH)_2$, $Mg(OH)_2$ and $CaMg.2(OH)_2$ as function of mixing and shaking at 250 rpm. The pH of the AMD sample (2.56) treated in this study indicates that it contains high levels of sulphate; as Feng et al. (2004) stated that a pH around 2.0 is of such a nature. The discussion about the pH changing trend is based on the double layer compression of aqueous colloids and ionic strength of the metal hydroxide added to the AMD sample. These two factors play a pivotal role in the destabilization-hydrolysis of the aqueous colloids-metal ions. In the present study the destabilization effect of the metal hydroxide during the AMD treatment is

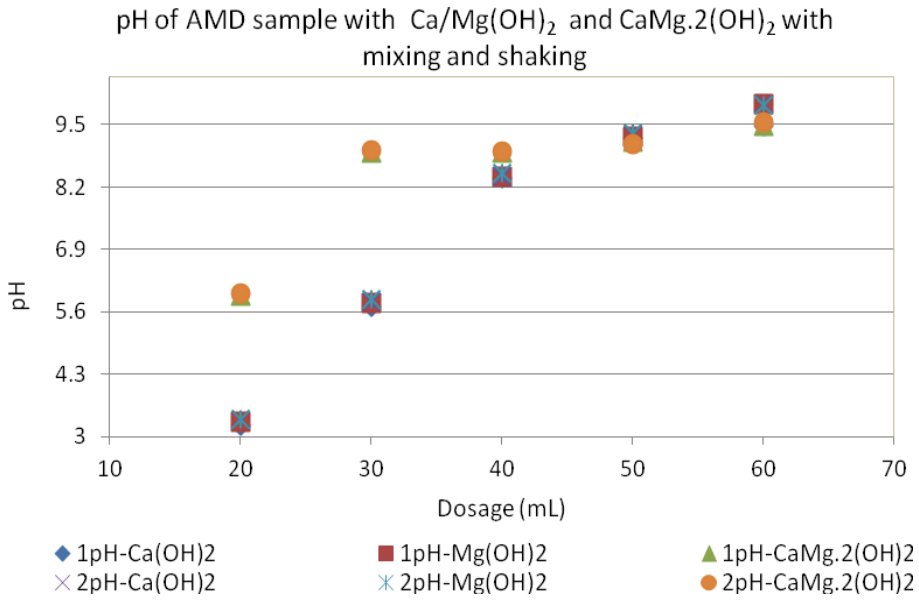

Figure 2. pH of AMD with $Ca(OH)_2$, $Mg(OH)_2$ and $CaMg.2(OH)_2$ with mixing and shaking. (1pH = pH with mixing and 2pH = pH with shaking).

introduced, a concept which is only associated with metal salts and polymers. It is obvious that the metal ions of the metal hydroxides, namely Ca^{2+} and Mg^{2+} undergo hydrolysis reaction in a similar manner to the Fe^{3+} and Al^{3+} ions in their respective metal salts. The difference between the metal ions in the hydroxides and metal ions in the metal salts is that the former are depicted to have less electronegativity compared to the latter (valence electrons). Explicit chemical reactions which occur in the AMD sample with metal hydroxide dosage will be elaborated under the discussion of the residual turbidity.

Although the studies carried out by Geldenhuys et al. (2001), Naicker et al. (2003), Maree (2004), Semerjian and Ayoub (2003), Watten et al. (2005), Akcil et al. (2006), Kurniawan et al. (2006), Herrera et al. (2007) and Sibrell et al. (2009) stated that the addition of the metal hydroxide to acidic wastewater (AMD) is for the OH^- ions to neutralize the solution and to form precipitates of metal hydroxide with the heavy metals. This study however explains the effect of the added metal hydroxides to the wastewater is explained as of destabilizing the colloidal suspension and form hydrolysis species. Figure 1 shows the configuration of the double layer, a region which is concentrated with counter-ionic charges which cause the stability in the colloidal suspension. Literature by Hubbell and Clark (2003), Binnie et al. (2003), Amuda et al. (2006), Ghaly et al. (2006) and Kurniawan et al. (2006) only mentions the parameters of the pH within which coagulation-flocculation is optimal, and nothing about the effect of the destabilization on the pH changing trend.

In this study, a hypothetically confirmation that poor destabilization yields poor turbidity removal will be an indication of ineffective rate of hydrolysis (poor flocs formation to adsorb/absorb turbid materials). The addition of metal hydroxides (coagulants) resulted in the destabilization of the AMD sample, thereby enabling the oxidation of FeS_2 when it reacted with water and dissolved oxygen to form Fe^{2+}. The Fe^{2+} is further oxidized by residual dissolved and atmospheric oxygen to form Fe^{3+} ions as shown by Equations 1 and 2. It clearly indicates that the Fe^{3+} ions undergo through hydrolysis process to form the precipitates of $Fe(OH)_3$ species. These precipitates remove turbid materials in the form of flocs, carbonate or oxide containing materials, up to a pH of minimum solubility (~4.0). Any residual FeS_2 in the treated AMD sample are also adsorbed by the precipitates ($Fe(OH)_3$). Ferric ions are relatively easy to remove from the AMD sample because they start to precipitate at a pH as low as 3.0 (Maree et al., 2003). Ferrous hydroxides do not settle as well as ferric does, and that can create a highly viscous sludge (Aubé and Arseneault, 2003). Although the molar solubility product constant of ferrous hydroxide is relatively small (American Water Works Association, 1995), removal is dictated by pH (Labuschagne et al., 2005). Precipitation is slow and incomplete at pH values less than 7.5.

The first step which occurs when $Ca(OH)_2$ and $Mg(OH)_2$ are added to an AMD sample is the dissolution to form solvated M^{2+} and OH^- species, where the latter causes neutralisation of the reaction. The OH^- ions increase the pH of the solution as shown by Equation 16. The two following equations illustrate these reactions:

$$M(OH)_2 \rightarrow M^{2+}{}_{(aq)} + 2\ OH^- \quad (M = Ca \text{ or } Mg) \tag{16}$$

The OH^- ions combine with the dissolved heavy metals to

produce precipitates ($M(OH)_2$ or $M(OH)_3$). The Fe and Al are two metal ions which are trivalent and form ($Fe(OH)_{3(s)}$ or $Al(OH)_{3(s)}$) hydrolysis species (complexes form during hydrolysis), whereas bivalent metals such as Co, Cu, Ni, Pb, Mn, Pb, Zn, Sb and Se react with OH^- which are derived from the bipolar water molecules ($H^{\sigma+}$-$OH^{\sigma-}$) or metal hydroxide to form ($M(OH)_2$), a reverse reaction of Equation 16. The concentration of some of the metals found in the AMD is very low, hence are not included in Table 5. The Ca^{2+}, Mg^{2+}, Mn^{2+} and Na^+ which dissolve in the solution and add to conductivity; which in some cases it is low; showing to be reacting in the system. This depicts that the Ca^{2+} and Mg^{2+} ions added to AMD sample do not only neutralize the solution but also play a role during destabilization; whereas the OH^- ions increases the pH of the system as well as form precipitates with metal ions. The precipitates are either adsorbed onto the polymers or settle to form sludge. The inference is based on the reduced concentration of metals as shown by the concentration of the metals in untreated and the treated AMD samples (Table 2).

The pH increasing trend (Figure 2) indicates that there is an addition of OH- to the samples with increasing dosage of $Ca(OH)_2$, $Mg(OH)_2$ and $CaMg.2(OH)_2$ respectively. According to Equation 1, the pH recedes during hydrolysis, as speciation occurs when the slightly negative hydroxyl ($OH^{\sigma-}$) of the water molecule pulls the H^+ of a water molecule which surrounds the central metal ion (Equation 17). The water molecule (latter) is detached from the central metal ion and replaced by the same slightly negative hydroxyl, causing reduction of the hexagonally-hydrated central metal ion from M^{3+} valence to M^{2+} (Equation 17). The dehydration continues until the hexagonally-hydrated metal ion reaches equilibrium state (dehydrated and insoluble), thus forming a precipitate (Equation 3). On the other hand, the reagent (proton donor or acceptor) reacts to either rise or reduce the pH of the solution (AMD sample). It is however, envisaged to obtain a pH rising trend because of the metal hydroxide added to the AMD samples, if only the concentration of the OH^- released exceeds that of the protons released during hydrolysis. This can be observed from the higher pH values of the AMD samples with synthetic $CaMg.2(OH)_2$ dosage, because for every 2 moles of OH^- released by $Ca(OH)_2$ or $Mg(OH)_2$, there are 4 moles of OH^- released by synthetic $CaMg.2(OH)_2$. It must also be noted that the rate of hydrolysis is determined by the reactivity potential of a coagulant/flocculent, as high valence electrons (M^{2+} or M^{3+}) yield a better destabilization-hydrolysis potential (Spellman, 2009). On the other hand, the OH^- from the metal hydroxides can still be utilized to remove some heavy metals in wastewater (AMD) to form insoluble $M(OH)_{2(s)}$. The utilization of the OH^- in this phenomenon is determined by the numerical value and the concentration of the metals in the solution. It is therefore very clear that in the current application (Figure 2), both the numerical value and the concentration of the metals are low, hence the remaining OH^- could manage to neutralize the H^+ and the excess proliferated the pH in the AMD samples as the dosage increased.

$$[M(H_2O)_5(H_2O)]^{3+} + H^{\delta+}\text{-}OH^{\delta-} \rightarrow [M(H_2O)_5(OH)]^{2+} + H_3O^+ \quad (17)$$

The difference of the pH values obtained in the corresponding AMD samples with all the three types of reagents ($M(OH)_2$) is insignificant. Their neutralization potential proliferated the pH of the AMD from 2.56 to a range of 3.23 to 9.9 (Figure 2), and a neutralizing potential of a range 20.7 to 74.1%. Their pH changing trend is uniform except in the samples with 20 mL of $CaMg.2(OH)_2$ dosage treated with mixing and shaking (5.93 and 5.98) compared to 3.23, 3.3, 3.34 and 3.36 with 20 mL of $Ca(OH)_2$ and $Mg(OH)_2$ dosage. The 2 moles of OH^- in $CaMg.2(OH)_2$ are equivalent to 1 mole in $Ca(OH)_2$ or $Mg(OH)_2$, because they calculated from 0.021 M of Ca^{2+} in $Ca(OH)_2$ and 0.021 M of Mg^{2+} in $Mg(OH)_2$ to make up 0.043 M of a former compound.

The ionic strength of a solution determines the neutralization potential of the metal ions in a coagulant/flocculent, a determinant of destabilization-hydrolysis. Higher ionic strength leads to higher rate of precipitation and vice versa, that is, high ionic strength has lower electrostatic potential and higher van der Waals forces of attraction. This results in higher rate of destabilization and it is calculated in Equation 18:

$$I = 0.5 \times \Sigma C_j Z_j^2 \quad (18)$$

C_j = concentration of the jth species (mole/L) and Z_j^2 = valence (or oxidation) number of the jth species. The ionic strength of both Ca^{2+} and Mg^{2+} (with C_j = 0.043 M and Z_j^2 = 4) is 0.086 each and in combined CaMg is 0.084 (~ 0.1). These values are slightly less than that of a trivalent Fe^{3+} (0.196), as observed in the study by Ntwampe et al. (2014) where an AMD sample was dosed with 0.043 M Fe^{3+} in $FeCl_3$ or $Fe_2(SO_4)_3$ yielded similarly equal residual turbidity (<10 NTU) to that with Ca^{2+} and Mg^{2+} hydroxides. Equation 18 can be used to calculate the activity coefficient (γ) of Ca^{2+} and Mg^{2+} as shown in Equation 19:

$$Log\ (\gamma) = \frac{0.5\,(Z_i^2)\sqrt{I}}{1+\sqrt{I}} \qquad \gamma = 10^{-\log(\gamma)} \quad (19)$$

By applying Equations 18 and 19, the calculations were found to be identical (both z = 2) for both Ca^{2+} and Mg^{2+}, which confirms the pH values obtained in Figure 2. This indicates that the rate of destabilization depends upon the ionic strength of the metal ions in a metal salt. This also supports the hypothesis (of this study) that destabilization and hydrolysis co-exist; which also indicates that destabilization occurs on the aqueous

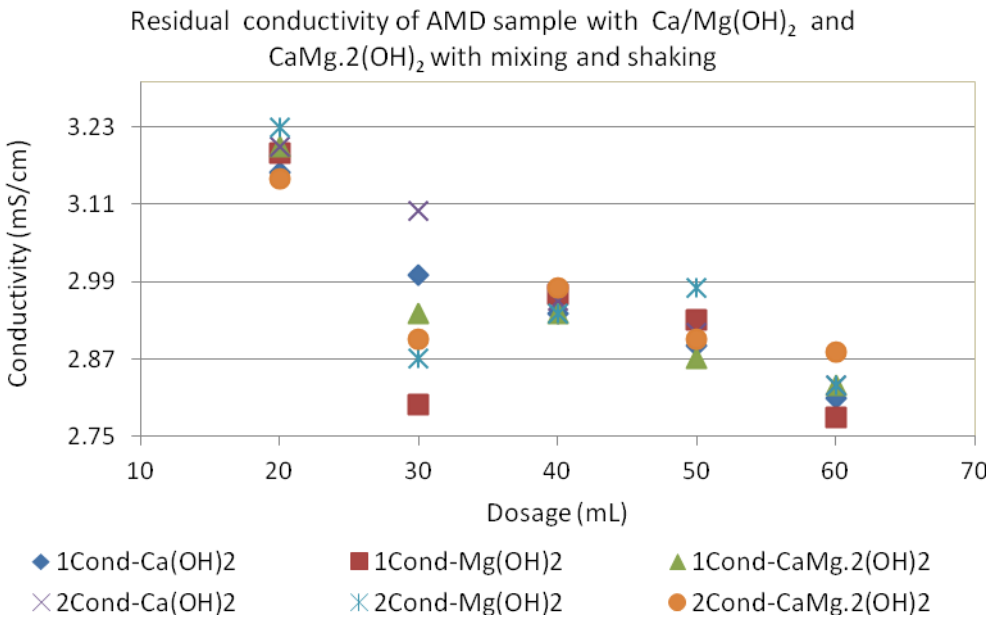

Figure 3. Conductivity of AMD with $Ca(OH)_2$, $Mg(OH)_2$ and $CaMg.2(OH)_2$ with mixing and shaking. (1cond = conductivity with mixing and 2cond = conductivity with shaking).

colloids, whereas hydrolysis occurs on the metal ion (M^{n+}) of the coagulant(s). Although ionic strength of a metal ion in a metal salt can be identical to that of a metal ion in a metal hydroxide, their performance in wastewater is influenced by the pH status of the system (acidic or basic). This inference is based on the difference which may be caused by Z_i^2 values between trivalent and divalent in Equation 18.

The conductivity changing trend shows an inconsistent changing (decreasing) behaviour (Figure 3) as the dosage increases, except for $Ca(OH)_2$, a condition which will be explained later. The reduction in the conductivity in the AMD sample with $Ca(OH)_2$ and $Mg(OH)_2$ dosage indicates high inevitability of $Mg(OH)_{2(s)}$ and $CaSO_4.2H_2O_{(s)}$ formation, (Equations 11 and 12). The addition of $Mg(OH)_2$ causes the destabilization of the AMD sample, resulting in the oxidation of Fe^{2+} (FeS_2) to form $Fe(OH)_{3(s)}$ (Equation 3). The $Ca(OH)_2$ reacts with the SO_4^{2-} ions which were formed during the oxidation reaction of FeS_2 (Equation 9) to form the precipitate of $CaSO_4.2H_2O$ (gypsum). These reactions involve the consumption of Ca^{2+} and Mg^{2+} ions added to the AMD sample, thus causing a decrease in their concentration. This implies that Fe^{2+} in FeS_2 is a limiting agent, and the addition of Ca^{2+} or Mg^{2+} to AMD must be stoichiometric in order to avoid water hardness due to over-dosage. It is concluded that the conductivity of the $Mg(OH)_2$ dosage does not have a direct relationship with the pH, but the $Ca(OH)_2$ does because of the consumption of SO_4^{2-} ions. This is confirmed by the uniform decreasing trend of the conductivity with increasing dosage (Figure 3).

Turbidity below 15 NTU is regarded as acceptable based on the low value obtained from the AMD sample (100 NTU). Turbidity removal in all the samples with 30 to 60 mL dosage is in the range of 88.7 to 97.5 NTU, a removal efficiency of 88.7 to 97.5% (Figure 4). A 20 mL dosage of the three reagents in the AMD samples yielded a slightly poorer turbidity removal in the range of 72.6 to 78.9, removal efficiency of 72.6 to 78.9% (Figure 4). Since it has been mentioned above that the reaction between the metal hydroxide (reagents) and the Fe^{2+} in FeS_2 is stoichiometric, it thus indicates that the turbidity removal values obtained with 20 mL dosage reflect under-dosage. The effect of under-dosage causes partial destabilization of the counter-ionic charge of the colloidal suspension, a condition in which a reduction of electrostatic forces of repulsion is implicit, causing incomplete destabilization of van der Waals forces-electrostatic repulsive forces (Swartz et al., 2004). Such a condition tends to minimize the oxidation efficiency of Fe^{2+} in FeS_2 which results in a low concentration of the flocs formation ($Fe(OH)_{3(s)}$).

According to existing literature by Azapagic (2004), Peppas et al. (2000), Kuyucak (2001 and 2002), Semerjian and Ayoub (2003), Maree (2004), Sibrell et al. (2005), Watten et al. (2005) and Herrera et al. (2007), the $Ca(OH)_2$ and $Mg(OH)_2$ neutralize FeS_2, where the former reacts with the SO_4^{2-} ions to form insoluble $CaSO_4.2H_2O$. After these metal hydroxide are added to AMD sample, destabilization occurs and the Fe^{2+} ions (FeS_2) undergo a hydrolysis process to form the precipitates (flocs) of ferric hydroxide ($Fe(OH)_{3(s)}$), including the likelihood of reduction-oxidation. The unreacted Fe^{2+} ions also undergo a hydrolysis process to form unstable $Fe(OH)_2$ species. Both ferrous and ferric hydroxide species act as adsorption substrate and removal of the residual turbid

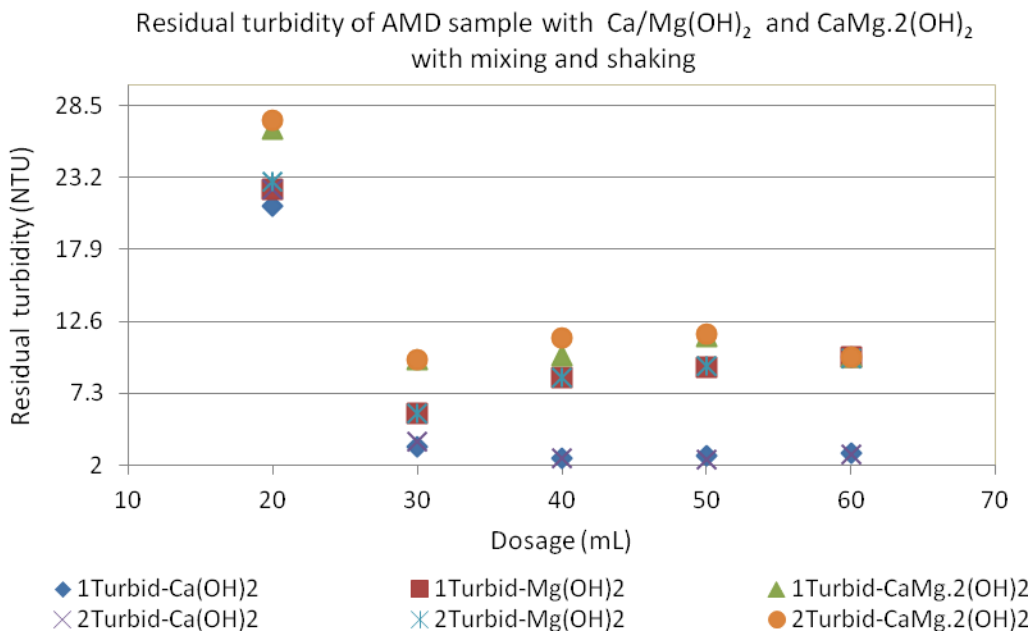

Figure 4. Turbidity of AMD with $Ca(OH)_2$, $Mg(OH)_2$ and $CaMg.2(OH)_2$ with mixing and shaking. (1turb = turbidity with mixing and 2turb = turbidity with shaking).

materials due to their porous property. Their sponge-like structure causes further adsorption when settling due to the higher settling velocity (Ntwampe et al., 2013).

The metal hydroxides perform the same function as metal salts except for the fact that OH^- forms an anionic component in the former reagent, whereas Cl^- and SO_4^{2-} form in the latter. In order for an optimal turbidity removal to occur (Figure 4), the coagulants must possess a high chemical potential so as to disturb electroneutrality in the system (double layer compression), which results in destabilization of the solution. The colloidal particles then collide with their neighbouring particles into settleable flocs. The electrostatic interactions in the EDL control many properties of mineral surfaces as well, as the interactions between them: that is, phase equilibrium, coagulation, aggregation, sedimentation, filtration, catalysis reaction and ionic transport in porous media, hence a choice of a coagulant with a high chemical potential is essential. According to the physico-chemical properties of the reagents in Table 1 (Wulfsberg, 1987), the pk_b, electronegativity, Z^2/r and atomic radii are compatible to both Ca and Mg.

The turbidity removal between the samples with mixing and their corresponding samples with shaking is identical. A combination of Ca and Mg to form a metal hydroxide compound $CaMg.2(OH)_2$ exhibit a relatively competitive performance when compared with $Ca(OH)_2$ and $Mg(OH)_2$. The advantage of using $CaMg.2(OH)_2$ in AMD is that both metal ions (Ca^{2+} and Mg^{2+}) are complementary as shown by Equations 11 and 12. The general reaction shown by those reactions indicate that both the cation- and anion- components solidify to form $CaSO_4.2H_2O$ and $Mg(OH)_2$, which also take part in the removal of Fe^{2+} through the formation of $Fe(OH)_{3(s)}$. The turbidity removal efficiency exhibited by Ca^{2+} and Mg^{2+} (Figure 3) is comparable to that shown by trivalent metal salts as stated by Water Specialist Technology (2003) and Hubbell and Clark (2003). The turbidity removal (Figure 4) corroborates the Schulze-Hardy rule which states that the valence ions with opposite charge to that of the sol determine the effectiveness of coagulation (Water Specialist Technology, 2003).

In view of the fact that one of the objectives in this study was to compare the turbidity removal between mixing and shaking, the results were satisfactory. However, the implications of collision frequencies (Equations 4 to 6) have been elucidated, but collision efficiencies of hydrodynamic forces seem corroborate shaking dynamics. In shaking method, rectilinear flow which is known for enhancement of rapid collision flow, is predominant compared to curvilinear flow. The former induces forward and backward collision of the colloidal particles per surface area whereas collision in a curvilinear flow (obtain in rapid mixing) is more likely to be deterred by the circular motion of the colloidal particles as there is less collision frequency (Atkins et al., 2006). Considering that the flocs compactness determines the rate of aggregation during wastewater treatment, this study recommends that shaking is an ideal technique to employ for chemical dispersion. This is because of the view that the flocs which are more compact are more likely to erode (loose size) during rapid

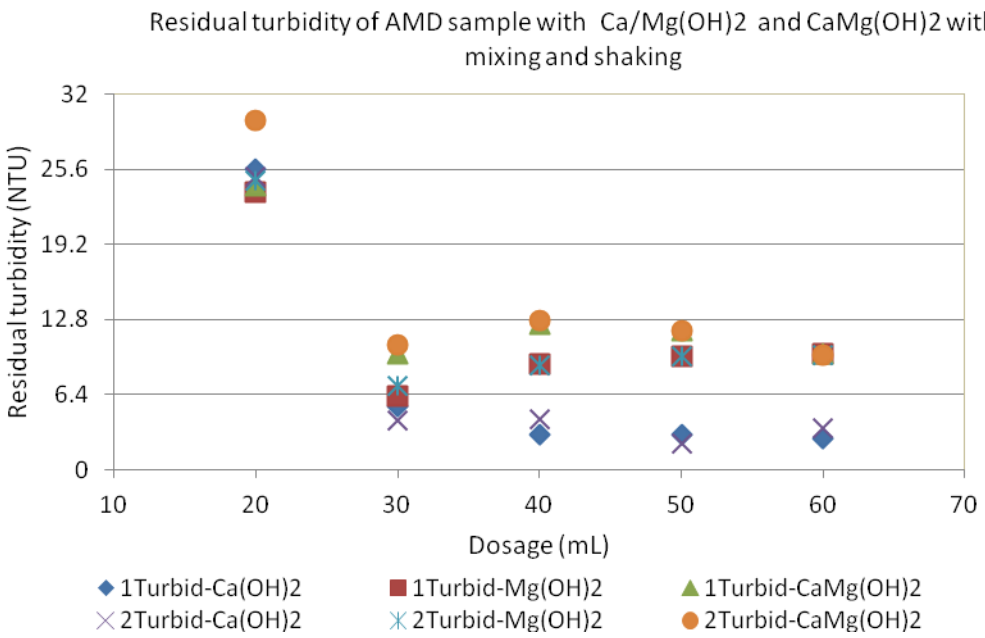

Figure 5. Turbidity of AMD with $Ca(OH)_2$, $Mg(OH)_2$ and $CaMg(OH)_2$ with mixing and shaking. (1turb = turbidity with mixing and 2turb = turbidity with shaking).

mixing whereas those less compact are fractured. These phenomena are common during nucleation where aggregation is induced by the adsorption of new flocs onto existing flocs.

A set of similar experiments was conducted by replacing $CaMg.2(OH)_2$ with $CaMg(OH)_2$ to determine the effect of the unpaired OH^- ions in the latter. The residual turbidity removal in the AMD sample with 20 mL $CaMg(OH)_2$ is similarly equal to the residual turbidity removal in the AMD sample with 20 mL $CaMg.2(OH)_2$. The residual turbidity removal in the AMD sample with 30 to 60 mL $CaMg(OH)_2$ dosage is slightly higher than in their corresponding samples with $CaMg.2(OH)_2$ as shown in Figure 4. The former yielded a residual turbidity in a range of 2.71 to 12.7 NTU whereas the latter yielded the residual turbidity removal in a range of 2.50 to 11.64 NTU. Equations 20 and 21 show the effect of the two reagents on the pH of the solution during dissociation process.

$$CaMg.2(OH)_2 \rightarrow Ca^{2+}_{(aq)} + Mg^{2+}_{(aq)} + 4\ OH^- \quad (20)$$

$$CaMg.2(OH)_2 \rightarrow Ca^{2+}_{(aq)} + Mg^{2+}_{(aq)} + 4\ OH^- \quad (21)$$

In Equation 20, there is an increase in the pH of the solution which occurs when the two OH^- ions are released and enhance the rate of hydrolysis when extra metal hydroxide species are formed compared to the speciation formed per one OH^- ion (Equation 21). It shows a deficiency of two hydrolysis species, which is the cause of a slight increase in the residual turbidity shown in Figure 5 (slightly lower turbidity removal). The hydrolysis species formed, depend upon the concentration of M^{3+}, ratio of moles of the OH^- added and moles of M^{3+} ions [OH]/[M] mole ratio, duration on hydrolysis of M^{3+} solution, anions in the solution, mixing mode of base with the M^{3+} solution and nature and strength of the base. The most predominant parameters which govern the nature of species are basic ratio, temperature and time (Jiang et al., 2012). Equations 20 and 21 express the relationship between speciation and the ratio of metal ions and hydroxide ions ([OH]/[M]) which can be expressed by the equilibrium state of hydrolysis using the concentration of H^+ (Equation 22).

$$M^{3+} + 3\ H_2O \rightleftharpoons \mathbf{M}(OH)_{3(s)} + 3\ H^+ \quad (22)$$

Where $n \leq 3$, the solubility behaviour of $M(OH)_3$ is expressed as K_{so} which describes the relationship between the concentrations of M^{3+} and H^+ in equilibrium with hydrous ferric oxides expressed as:

$$K_{so} = [M^{3+}][H^+]^3 \quad (23)$$

Since the experimental results have shown that there is a correlation between the pH and turbidity, the AMD samples with 20 mL of $Ca(OH)_2$, $Mg(OH)_2$ dosage show lower pH values and slightly higher residual turbidity compared to the $CaMg.2(OH)_2$ dosage (lower pH and slightly higher residual turbidity). Dosages above 20 mL show a uniform increasing trend of pH and a consistent residual turbidity value. It indicates that equilibrium during

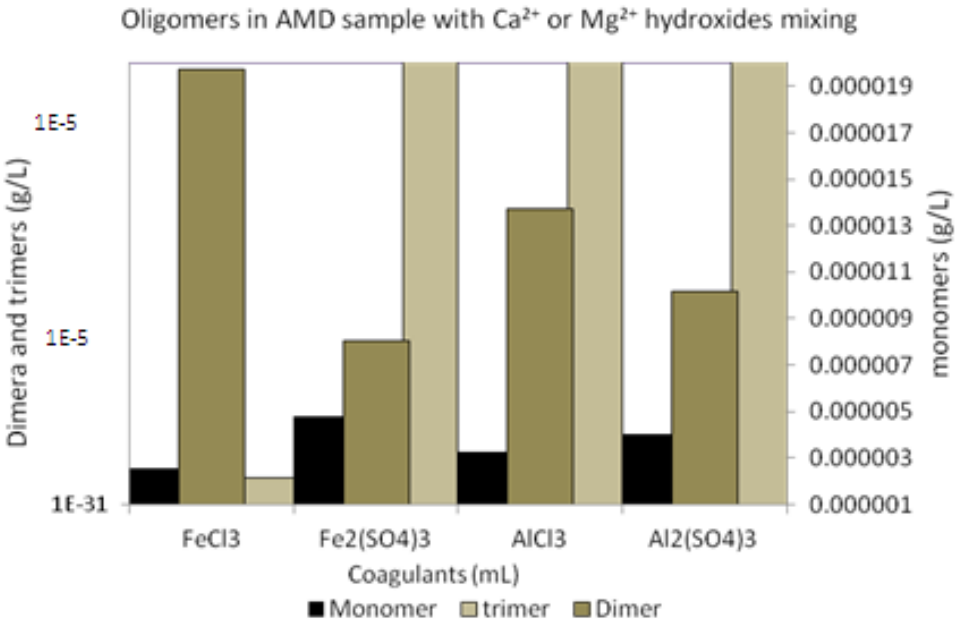

Figure 6. Oligomeric species in 30 mL of Ca^{2+} or Mg^{2+} hydroxide and CaMg.2(OH)2 salts in 200 mL AMD sample with mixing. (NB: The range of the primary Y-axis is 1.32E-20-1.66E-39).

destabilization-hydrolysis-adsorption was reached between 30 to 40 mL dosage and the extra dosage above that increased the pH of the solution. This also implies that the destabilization potential in Ca or Mg or a combination of CaMg is similarly equal. According to Equation 21, it is observed that the residual turbidity removal in the AMD sample with Ca^{2+} in $Ca(OH)_2$ or Mg^{2+} in $Mg(OH)_2$ or $CaMg.2(OH)_2$ dosage would be higher compared to Fe^{3+} in $FeCl_3$ or $Fe_2(SO_4)_3$. This merely indicates that the hydrolysis plays a major role in the AMD sample with $Ca(OH)_2$, $Mg(OH)_2$ or $CaMg.2(OH)_2$ compared to destabilization due to higher electronegative metal ions (Fe^{3+}). This simply implies that destabilization is at optimal point but slightly lower than in metal ions with high valence electrons; which then relies on hydrolysis as a complementary process. This occurs when the OH^- ions in metal hydroxides enhance hydrolysis reaction and increase the rate of flocs formation, thus increasing the adsorption process. The effective turbidity removal shown by $CaMg.2(OH)_2$ confirms that it can be used as a replacement of the $CaMg(CO_3)_2$ which has a limited pH increasing ability due to the buffering effect of CO_2.

In this study, the effect that hydrodynamic forces of the drag have upon the aggregates and the paths the aggregates follow as they approach one another is further investigated, which also plays a role on the effectiveness of the destabilization of the colloidal suspension.

Figures 6 and 7 show the oligomeric species formed during hydrolysis in the AMD sample with Ca^{2+} or Mg^{2+} hydroxides and $CaMg.2(OH)_2$ dosage with mixing and shaking respectively. Figures 6 and 7 showed similarly identical concentrations of trimeric (low) and monomeric species (higher) in both mixing and shaking, but the trimeric species with mixing are slightly higher compared to shaking.

Figures 8, 9 and 10 illustrate the correlation between the pH and the dosage, and that has been confirmed by the models, with the square of the correlations (R^2) above 95% in the AMD sample with $Ca(OH)_2$, $Mg(OH)_2$ and $CaMg.2(OH)_2$ dosage with shaking. The objective of plotting this technique was to check its efficiency for replacing a jar test method.

Figure 11 shows the SEM images of the AMD sludge samples with $Ca(OH)_2$, $Mg(OH)_2$ with shaking and $CaMg.2(OH)_2$ and $CaMg(OH)_2$ dosage with mixing and shaking respectively using 25000 magnification. The SEM images (Figures 11 and 12) show that turbidity removal is through adsorptive coagulation. This occurs when the destabilization is caused by adsorption of polymers or long hydroxide chains to the particle surface (Shen et al., 2007). Figure 11(A) showed larger-dense and a few small flocs joined together and settled on a solid sponge-like surface whereas Figure 11(B) showed small scattered flocs settling on a sludge-like solid surface. The SEM micrographs in Figure 12(A) showed small scattered flocs attached onto solid larger dense surfaces whereas Figure 12(B) showed larger and small flocs scattered throughout the slide with some voids in between.

Figure 13 shows the images of the AMD sludge with

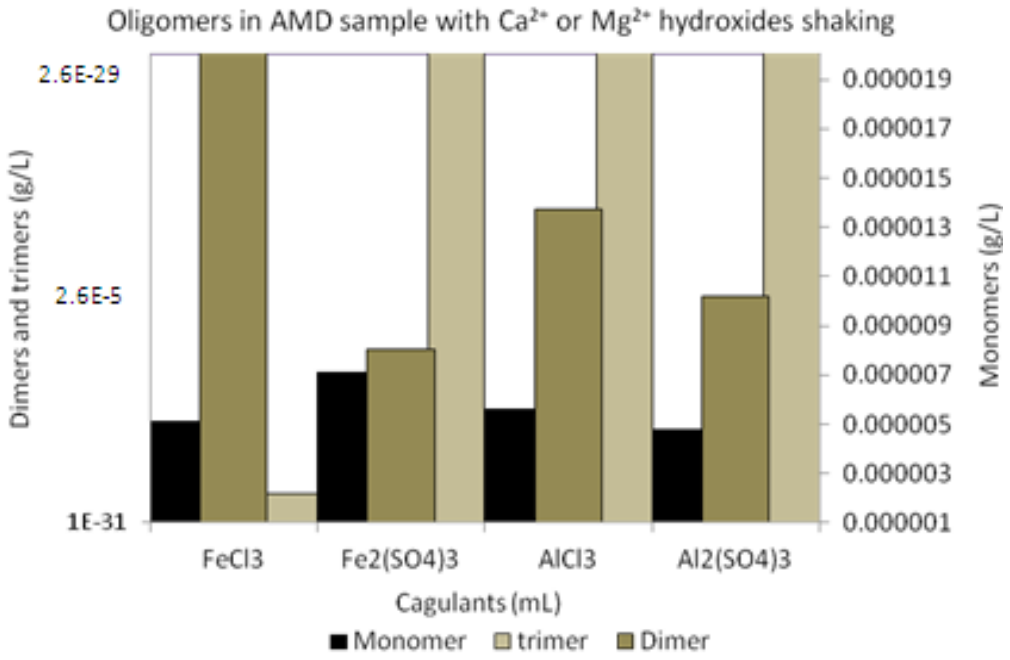

Figure 7. Oligomeric species in 30 mL of Ca^{2+} or Mg^{2+} hydroxide and CaMg.2(OH)2 salts in 200 mL AMD sample with shaking. (NB: The range of the primary Y-axis is 1.32E-20-1.66E-39).

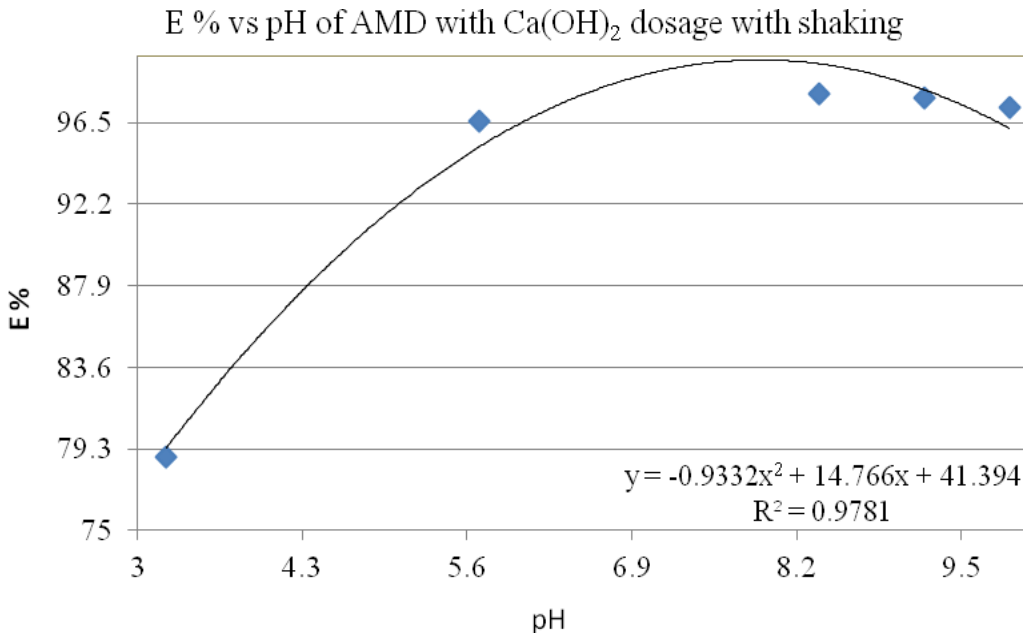

Figure 8. pH vs E % of 0.043 M $Ca(OH)_2$ with shaking.

$Ca(OH)_2$ and $Mg(OH)_2$ dosage with shaking respectively whereas Figure 14 shows the images of the AMD sludge with $CaMg.2(OH)_2$ and $CaMg(OH)_2$ mixing and shaking respectively. The results in Figures 13 and 14 show that the metal counts in the AMD sample with $Ca(OH)_2$ and $Mg(OH)_2$ shaking as well as $CaMg.2(OH)_2$ and $CaMg(OH)_2$ mixing and shaking respectively are similarly equal, showing Cu metal at 2000 counts and some unspecified metals around 1000 counts. The similarity in the values shown by the XRD patterns indicates that the

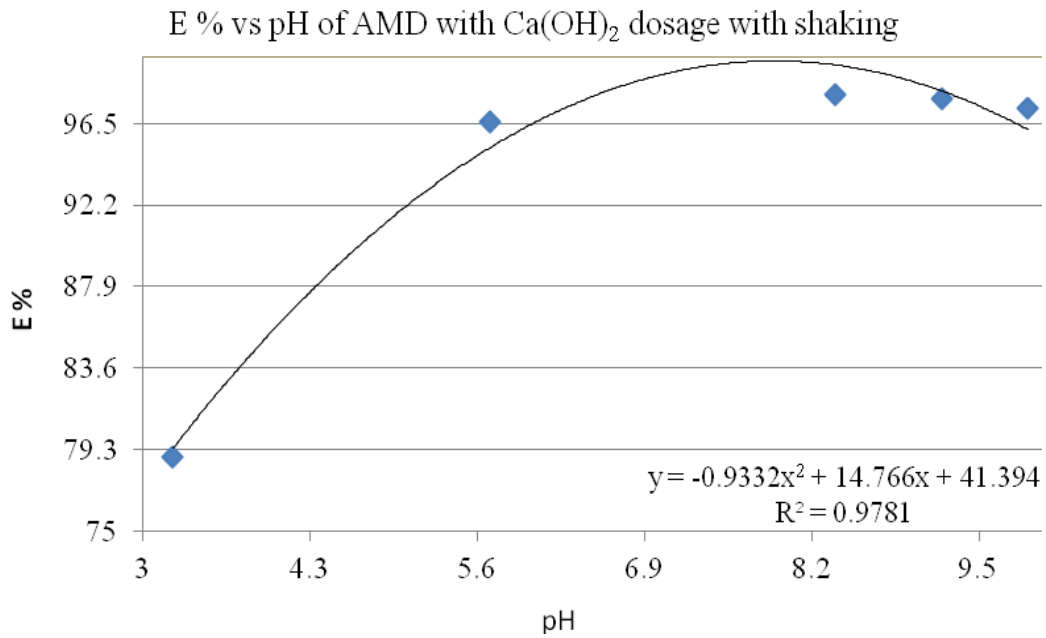

Figure 9. pH vs E % of 0.043 M $Mg(OH)_2$ with shaking.

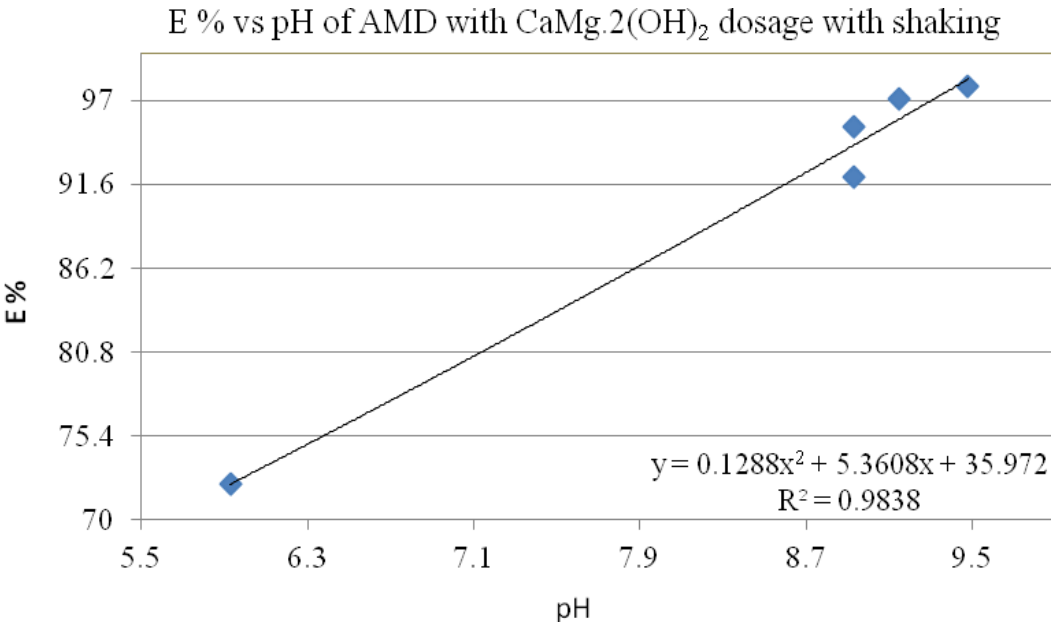

Figure 10. pH vs E % of 0.043 M $CaMg.2(OH)_2$ with shaking.

experiments on the AMD sample with $Ca(OH)_2$ or $Mg(OH)_2$ with mixing and shaking yield similar turbidity reduction potentials; a condition which also occurs in the AMD sample with $CaMg.2(OH)_2$ and $CaMg(OH)_2$.

The Pearson correlation coefficient (r) is used to calculate the relation between pH and residual turbidity. A correlation coefficient of 0.70 or higher is considered to be a very strong relationship, 0.40 to 0.69 a strong relationship, and 0.30 to 0.39 only a moderate relationship. The results of the experiments are used in the calculations below:

$\Sigma x_{M\text{-shaking}}$ = sum of pH during shaking, $\Sigma y_{M\text{-shaking}}$ =sum of turbidity removal during shaking, $\Sigma x^2_{M\text{-shaking}}$ = sum of the

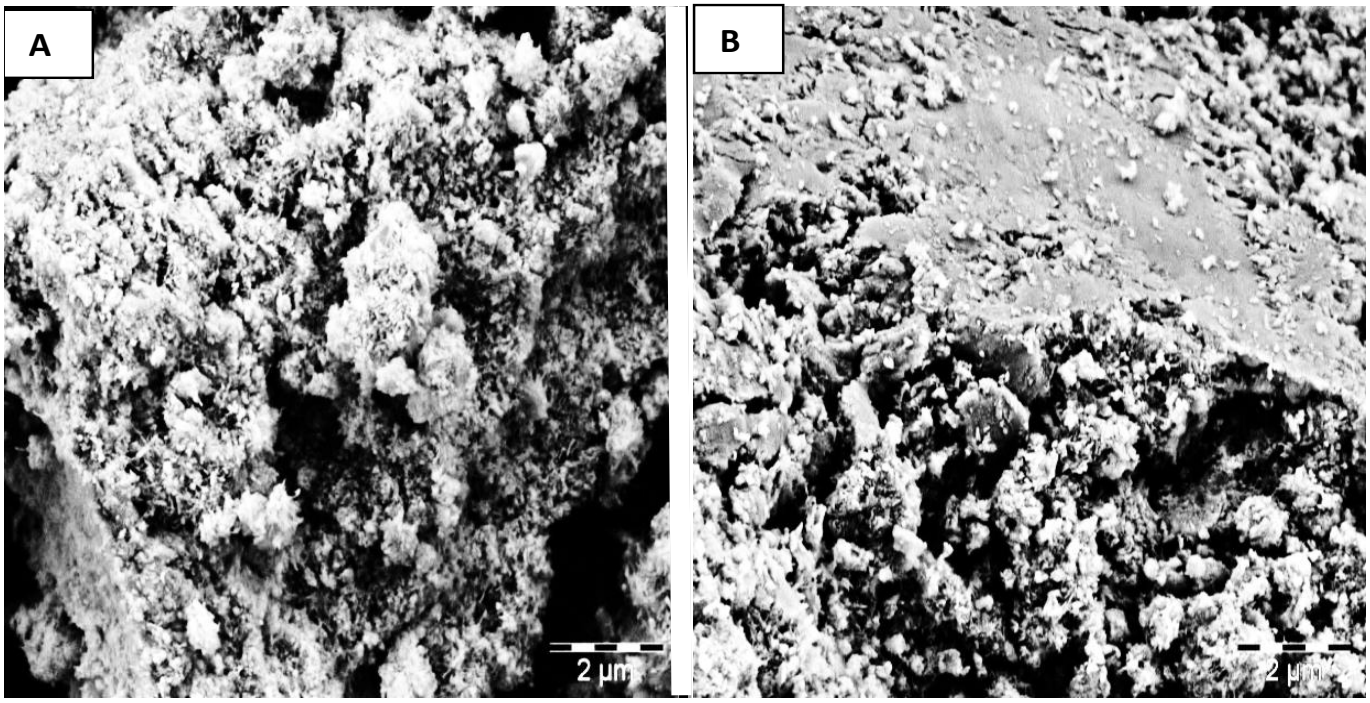

Figure 11. Comparison of SEM images between the sludge of the AMD with $Ca(OH)_2$ and $CaMg.2(OH)_2$ dosage with shaking (25000x).

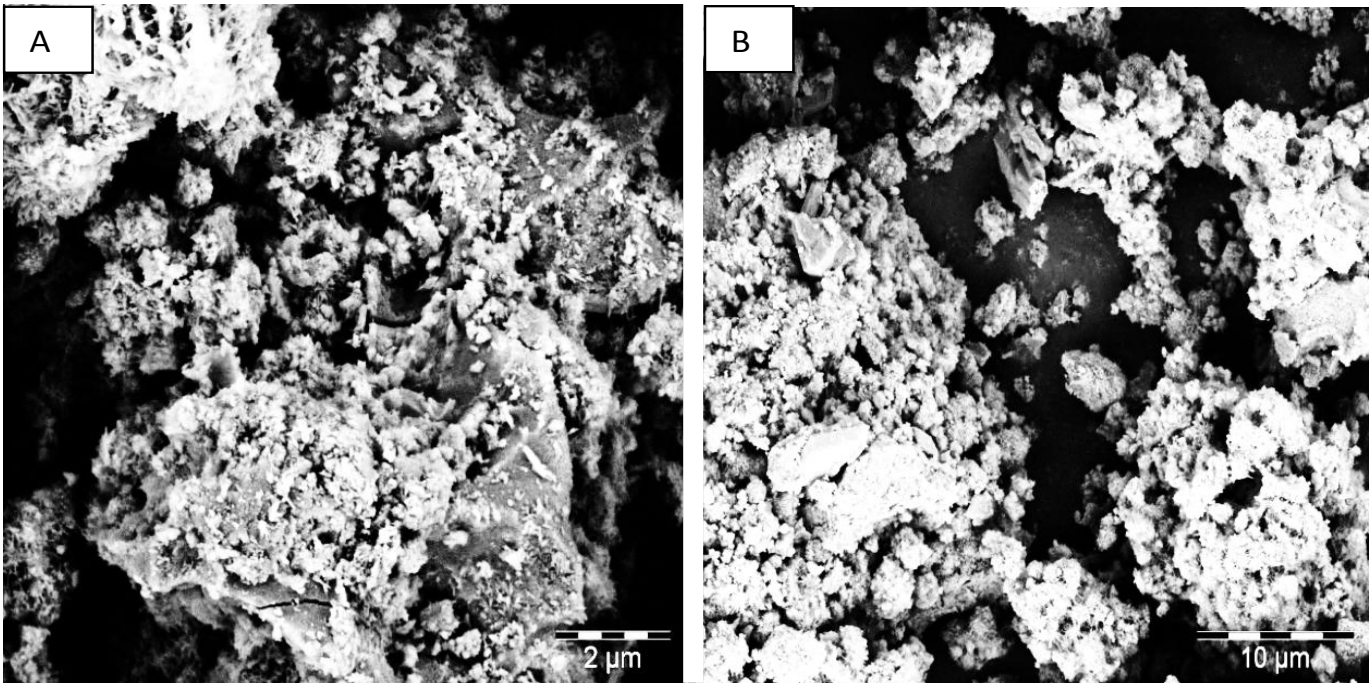

Figure 12. SEM images of the sludge in the AMD with $Mg(OH)_2$ and $CaMg.2(OH)_2$ dosage with shaking (25000x).

square of pH during shaking, $\Sigma y^2_{M\text{-shaking}}$ = sum of the square of turbidity during shaking and $\Sigma xy_{M\text{-shaking}}$ = sum of pH multiplied by sum of turbidity removal (M = Ca or Mg)

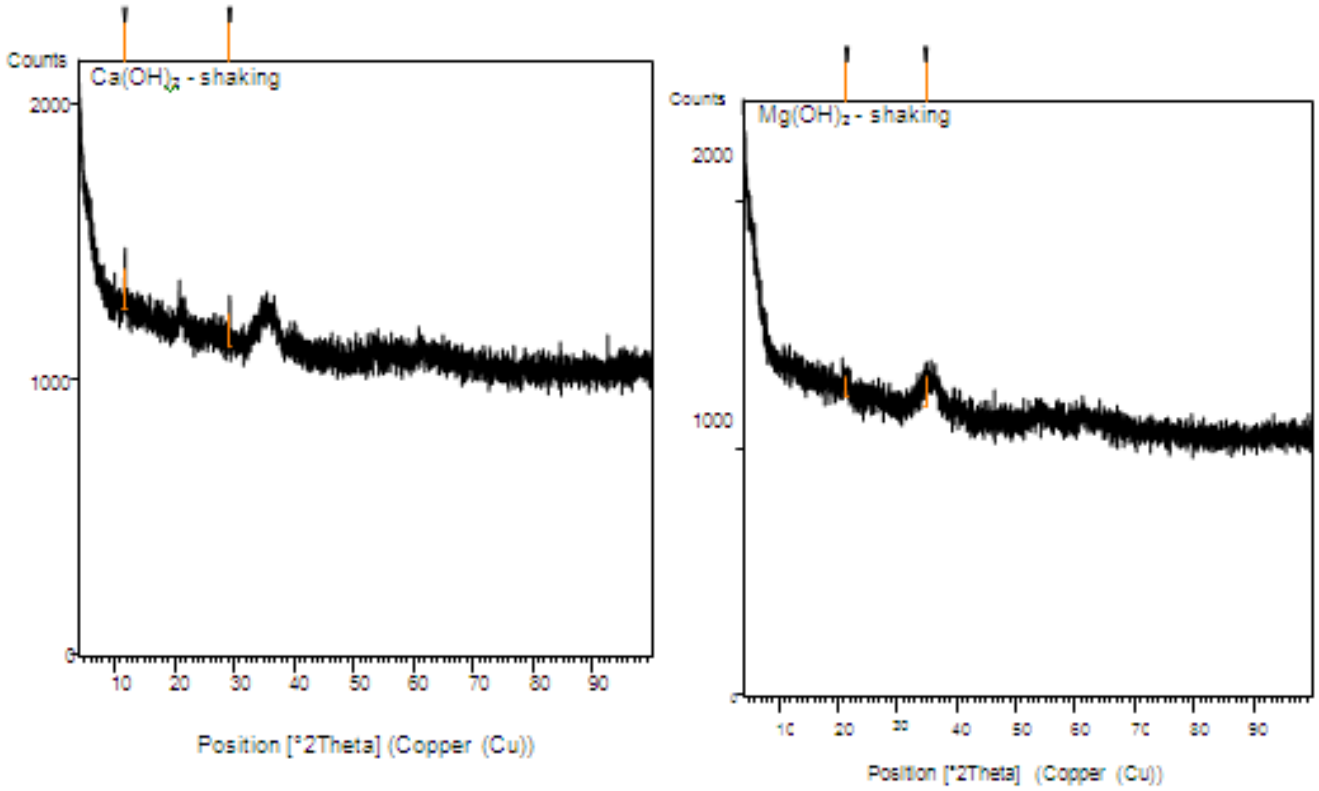

Figure 13. Residual copper in the AMD sludge with $Ca(OH)_2$ and $Mg(OH)_2$ dosage with shaking.

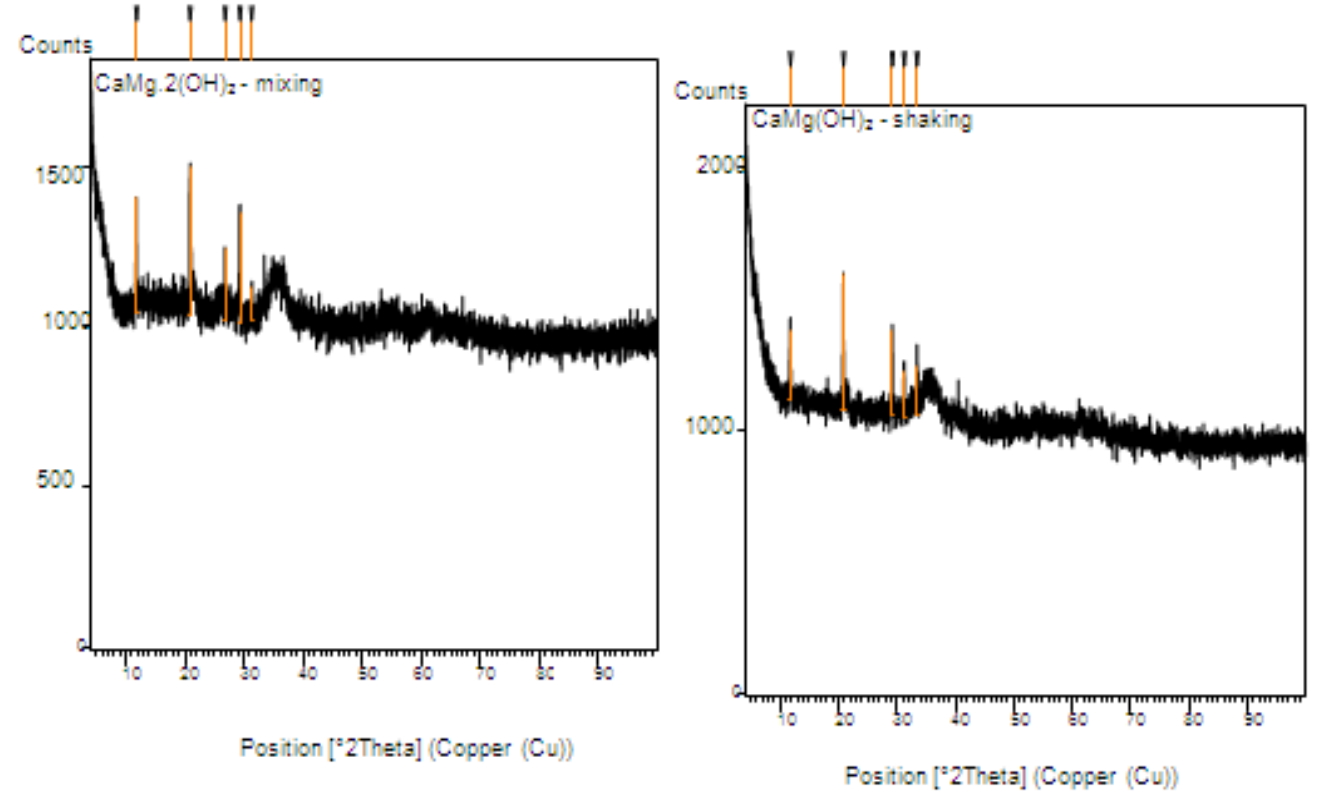

Figure 14. Residual copper in the AMD sludge with $CaMg.2(OH)_2$ dosage with shaking.

$\Sigma x_{Ca\text{-}shaking}$ = 36.4, $\Sigma x^2_{Ca\text{-}shaking}$ = 295.5, $\Sigma y_{Ca\text{-}shaking}$ = 31.4, $\Sigma y^2_{Ca\text{-}shaking}$ = 472.5 and $\Sigma xy_{Ca\text{-}shaking}$ = 151.4

$\Sigma x_{Mg\text{-}shaking}$ = 36.3, $\Sigma x^2_{Mg\text{-}shaking}$ = 291.2, $\Sigma y_{Mg\text{-}shaking}$ = 56.5, $\Sigma y^2_{Mg\text{-}shaking}$ = 815.5 and $\Sigma xy_{Mg\text{-}shaking}$ = 362.3

$\Sigma x_{CaMg\text{-}shaking}$ = 42.5, $\Sigma x^2_{CaMg\text{-}shaking}$ = 393.3, $\Sigma y_{CaMg\text{-}shaking}$ = 70.2, $\Sigma y^2_{CaMg\text{-}shaking}$ = 1209.1 and $\Sigma xy_{CaMg\text{-}shaking}$ = 554.4

Using the results obtained for the AMD sample with $Ca(OH)_2$ shaking, $Mg(OH)_2$ and shaking, and $CaMg.2(OH)_2$ shaking respectively, yielded r-values of 0.84, 0.72 and 0.50 (84.0, 71.7 and 50.0%) respectively. The range of the correlation coefficient is from -1 to 1 and the correlation coefficients calculated for the samples with shaking in the present experiment fall within a range of strong and very strong relationship. This is validated by all the R^2>98% values of the pH of $Ca(OH)_2$, and $Mg(OH)_2$ and $CaMg.2(OH)_2$ vs residual turbidity found in the treated AMD samples with shaking respectively as shown in Figures 5, 6 and 7, showing that the predictions obtained for the experimental data is considered to be satisfactory.

Conclusion

The turbidity removal efficiency exhibited by $Ca(OH)_2$ or $Mg(OH)_2$, and $CaMg.2(OH)_2$ is identical with all values >90%. Effective wastewater treatment is not necessarily dependent upon the pH but the ability of the coagulant to destabilize the double layer (high electronegativity) of the aqua-colloids coupled with optimal hydrolysis, precursor to adsorption. The Ca^{2+} and Mg^{2+} ions added to the AMD sample do not only neutralize the solution but also cause destabilization, whereas the anionic species (OH^-) increase the rate of speciation by reacting with metal ions and also increase the pH of the system. Increasing pH trend (Figure 2) indicates that there are some residual OH^- ions which did not react during the oxidation-neutralization-destabilization-hydrolysis chain reaction. Hydrolysis is a predominant process in AMD treatment with Ca^{2+} and Mg^{2+} hydroxide reagents impacting on the rate of destabilization. The conductivity of the $Mg(OH)_2$ dosage does not have a direct relationship with the pH, a condition exhibited by the $Ca(OH)_2$. A combination of 0.021 M Ca^{2+} in $Ca(OH)_2$ and 0.021 M Mg^{2+} in $Mg(OH)_2$ to form $CaMg.2(OH)_2$ exhibits a relatively competitive performance with 0.043 M Ca^{2+} in $Ca(OH)_2$ and 0.043 M Mg^{2+} in $Mg(OH)_2$, confirming that the former can be used as a replacement of $CaMg(CO)_3$. Turbidity removal in AMD with $Ca(OH)_2$, $Mg(OH)_2$ or $CaMg.2(OH)_2$ dosages is of a physical nature as observed from the SEM images which show the sponge cake-like structures with small and larger flocs bound together.

ACKNOWLEDGEMENTS

This work is based on the research financially supported by the South African Research Chairs Initiative of the Department of Science and Technology and National Research Foundation of South Africa (Coal Research Chair Grant No.: 86880, UID 85643, Grant No.: 85632). Any opinion, finding or conclusion or recommendation expressed in this research is that of the author(s) and the NRF does not accept any liability in this regard.

REFERENCES

Aboulhassan MA, Souabi S, Yaacoubi A, Baudu M (2006). Removal of surfactant from industrial wastewaters by coagulation flocculation process. Interf. J. Environ. Sci. Technol. 3(4):327-336.

Adams C, Wang Y, Loftin K, Meyer M (2002). Removal of antibiotics from surface and distilled water in conventional water treatment processes. J. Environ. Eng. 128(3):253-260.

Aguilar MI, Saez TSS, Liorens M, Soler A, Ortuno TSSF (2002). Nutrient removal and sludge production in the coagulation–flocculation process. Wat. Res. 36:2910-2919.

Aguilar MI, Suaez TSS, Liorens M, Soler A, Ortuno FV, Meseguer Fuentes A (2005). Improvement of coagulation-flocculation process using anionic polyacrylamide as coagulant aid: Chemosphere 55:47-56.

Akcil A, Koldas S (2006). Acid mine drainage (AMD): Causes, treatment and case studies. J. Cleaner Prod. 14(12-13):1139-1145.

American Water Works Association (AWWA) (1995). Water Treatment (second ed.), McGraw-Hill Publishers, USA, pp. 314-353.

Amuda OS, Amoo A, Ajayi OO (2006). Performance optimization of coagulant/flocculant in the treatment of wastewater from a beverage industry. J. Haz. Mat. 129:69-72.

Atkins P, de Paula TSS (2006). Physical Chemistry for the Life Sci. New York, NY: W.H. Freeman and Company.

Aubé B, Arseneault B (2003). “In-Pit Mine Drainage Treatment System in a Northern Ulmate” In Proceedings for Sudbbury Mining and Environ. Conference”, May 25-28 2003. (available at http://www.enviaubi.com/images/raglan.pdf).

Aubé B (2004). “Uneétude en usinepilote de la production de boues à haute densitédurant le traitement des eaux de drainage minieracide” {English Title: “A Pilot Studyof High Density Sludge Production inAcid MineDrainage Treatment”} Master’s thesis submitted to Université de Montréal – École polytechnique. April, 2004.

Aysegul P, Enis T (2002). Colour removal from cotton textile industry wastewater in an activate sludge system with various additives. Wat. Res. 36:2920-2925.

Azapagic A (2004). Developing a framework for sustainable development indicators for the mining and minerals industry. J. Cleaner Prod. 12(6):639-662.

Binnie C, Kimber M, Smethurst G (2003). Basic Water Treatment 3rd Ed, MPG Books, Bodmin, Great Britain.

Bolto B (2007). Organic polyelectrolytes in water treatment. Wat. Res. 41:2301-2324.

Carballa M, Omil F, Lema TSSM (2005). Removal of cosmetic ingredients and pharmaceuticals in sewage primary treatment. Wat. Res. 39:4790-4796.

Chang Q, Yu M (2004). An Application of macromolecular heavy metal flocculant in wastewater treatment. Chemosphere 6:42-47.

de Ridder D (2010). Modeling equilibrium adsorption of organic micropollutants onto activated carbon. Wat. Res. 44:3077-3086.

Dey MA. Hashim SH, Sen Gupta B (2004). Microfiltration of water-based paint effluent. Adv. Environ. Res. 8:455-466.

Diz HR (1997). Chemical and biological treatment of acid mine drainage for the removal of heavy metals and acidity, Ph.D. thesis, Virginia Polytechnic Institute and State University, USA.

Edwards AC, Withers PTSSA (2007). Linking phosphorus sources to

impacts in different types of water body. Soil Use Manage. 23:133-143.
Fasemore O (2004). The flocculation of paint wastewater using inorganic salts, A dissertation submitted for MSc degree at the University of the Witwatersrand, RSA.
Feng D, van Deventer S, Aldrich C (2004). Removal of pollutants from acid mine wastewater using metallurgical by-product slags. Sep. Purific. Technol. 40:61-67.
Freeze SD, Nozaic DJ, Pryor MJ, Rajogopaul R, Trollip DL, Smith RA (2001). Water Supply, vol. 1, IWA Publishing, SA.
Fu F, Wang Q (2010). Removal of heavy metal ions from wastewaters: A review. J. Environ. Man. pp. 407-418.
Ghaly AE, Snow A, Faber BE (2006). Treatment of grease filter washwater by chemical coagulation. Can. Biosyst. Eng. 48:6.13-6.22.
Goldberg S (2002). Competitive Adsorption of Arsenate and Arsenite on Oxides and Clay Minerals. Soil Sci. Soc. Am. 66:413-421.
Geldenhuys AJ, Maree JP, De Beer M, Hlabela P (2001). An integrated limestone/lime process for partial sulphate removal South African Institute of Mining and Metallurgy (SAIMM), 103(6):345-371.
Hankins N (2006). Enhanced removal of heavy metal ions bound to humic acid by polyelectrolyte flocculation. Separ. Purif. Technol. 51:48-56.
Herrera P, Uchiyama H, Igararashi T, Asakura K, Ochi Y, Iyatomi N, Nagae S (2007). Treatment of acid mine drainage through a ferrite formation process in central Hokkaido, Japan: Evaluation of dissolved silica and aluminium interference in ferrite formation. Miner. Eng. 20:1255-1260.
Hubbell R, Clark C (2003). Upper Clinton Sub-watershed Management Plan: for the city of Michigan prepared by Upper Clinton Sub-watershed Core Group, USA.
Jiang J-Q, Stanford C, Mollazeinal A (2012). Application of ferrate for sewage treatment pilot to full scale trials. Globa NEST TSS 14(1):93-99.
Kalin M, Fyson, Wheeler WN (2006). The chemistry of conventional and alternative treatment systems for the neutralization of acid mine drainage. Sci. Tot. Environ. 366(2-3):395-408.
Kempkes M, Eggers J, Mazzotti M (2007). Measurement of particle size and shape by FBRM and *in-situ* microscopy. Chem. Eng. Sci. doi: 10.1016/TSSces.2007.10.030
Kurniawan TA, Chan WS, Lo W-S, Babel S (2006). Physico-chemical treatment techniques for wastewater laden with heavy metals. Chem. Eng. 118:83-87.
Kuyucak N (2001). Acid Mine Drainage – treatment options for mining effluents. Mining Environ. Man. pp. 14-17.
Kuyucak N (2002). Role of microorganisms in mining: generation of acid rock drainage and its mitigation and treatment. Euro. J. Min. Proc. Environ. Protect. 2(3):179-196.
Labuschagne PF, Usher BH, Matfield F (2005). Geohydrological management approaches for site closure in South African gold mines. In: Proceedings of 2nd International Conference on Processing and Disposal of Minerals Industry Wastes (PDMIW 05), Falmouth, UK.
Li SS, Hoggins DO (2010). Modelling wastewater effluent mixing and dispersion in a tidal channel. Can. J. Civil Eng. 37(1):99-111.
Maree JP, Greben H, De Beer M (2004a). Treatment of acid and sulphate-rich effluents in an integrated biological/chemical process. Water SA, 30(2):183-190.
Maree JP (2004b). Treatment of industrial effluent for neutralization and sulphate removal, A thesis submitted for PhD at the North West University, RSA.
Wang LK, Vaccari DA, Li Y, Shammas NK (2004). Chemical Precipitation. In: Wang, L.K., Hung, Y.T. and Shammas, N.K., Eds., Physicochemical Treatment Processes, Vol. 3, Humana Press, New Jersey, pp. 141-198.
McCurdy K, Carlson K, Gregory D (2004). Floc morphology and cyclic shearing recovery: comparison of alum and polyaluminum chloride coagulants. Wat. Res. 38(2):486-494.
Metcalf W, Eddy C (2003). Wastewater Engineering. 4th, McGraw-Hill Inc, New York.
Naicker K, Cukrowska E, McCarthy TS (2003). Acid mine drainage arising from gold mining activity in Johannesburg, South Africa and environs. Environ. Pol. 122:29-40.
Ntwampe IO, Jewell LL, Glasser D (2013). The effect of water. hardness on paint wastewater treatment by coagulation-flocculation. J. Environ. Chem. Ecotox. 5(1):7-16.
Ntwampe IO, Waanders FB, Fosso-Kankeu E, Bunt JR (2014). Reactivity of Fe salts in the destabilization of acid mine drainage employing mixing and shaking techniques without pH adjustment. Intern. J. Mat. Proct.
Peppas A, Komnitsas K, Halikia I (2000). Use of organic covers for acid mine drainage control. Min. Eng. 13(5):563-574.
Pratt C, Shilton A, Pratt S, Haverkamp RG, Elmetri I (2007). Effects of redox potential and pH changes on phosphorus retention by melter slag filters treating wastewater. Environ. Sci. Technol. 4(18):6583-6590.
Scherrenberg SM, Menkveld HWH, Schuurman DJ, den Elzen JJM, van der Graaf JHJM (2008). Advanced treatment of WWTP effluent; no use or reuse? Wat. Pract. Technol. 3(2).
Semerjian L, Ayoub GM (2003). High-pH-magnesium coagulation-flocculation in wastewater treatment. Adv. Environ. Res. 7:389-403.
Shen M, Xu X, Wang Y, Guo Y, Fan M, Tan G (2007). Relationship Between the Polymer Structures and Destabilization of Polymer-Containing Water-in-Oil Emulsions. J. Dispers. Sci. Technol. 28:1178-1182.
Sibrell PL, Montgomery GA, Ritenour KL, Tucker TW (2009). Removal of phosphorus from agricultural wastewaters using adsorption media prepared from acid mine drainage sludge. Wat. Res. 43(8):2240-2250.
Sincero AP, Sincero GA (2003). Physical-chemical treatment of water and wastewater IWA Publishing, Londao, USA.
Spellman FR (2009). Handbook of water and wastewater treatment plant operations, CRC Press, USA.
Suarez S, Lerna JM, Omil F (2009). Pre-treatment of hospital wastewater by coagulation-flocculation and flotation. Bioresour. Technol. 100(7):2138-2146.
Swartz CD, Morrison IR, Thebe T, Engelbrecht WJ, Cloete VB, Knott M, Loewenthal RE, Kruger P (2004). Characterisation and Chemical Removal of Organic Matter in South African Coloured Surface Waters. WRC Report No. 924/1/03. Water Research Commission, Pretoria, South Africa.
Tchobanoglous G, Burton FL, Stensel HD (2003). Wastewater Engineering Treatment and Reuse, 4th, Ed, Metcalf & Eddy Inc.
Van der Graaf JHJM, Geilvoet SP, Roorda J (2010). Particle characterisation related to membrane filtration of wastewater: Handbook on Particle Separation Processes, IWAPublishing Editor(s): Arjen Van Nieuwenhuijzen and Jaap Van der Graaf ISBN: 9781843392774.
van Nieuwenhuijzen (2002). Scenario Studies into Advanced Particle Removal in the Physical-Chemical Pre-Treatment of Wastewater 2002 PhD-thesis Delft University of Technology, DUT Press, ISBN 9040722498.
Water Specialist Technology (2003). Jar test procedure for precipitants, coagulants and flocculants, Florida, USA.
Watten BJ, Sibrella PL, Schwartz MF (2005). Acid neutralization within limestone sand reactors receiving coal mine drainage. Environ. Pol. 137:295-304.
Wulfsberg G (1987). Principles of Descriptive Inorganic Chemistry, Brooks/Cole Publishing Company.